Biophysical Journal
Article

Biophysical Society

Analysis of L-DOPA and droxidopa binding to human β_2-adrenergic receptor

Akash Deep Biswas,[1] Andrea Catte,[1,*] Giordano Mancini,[1] and Vincenzo Barone[1,*]
[1]Scuola Normale Superiore, Pisa, Italy

ABSTRACT Over the last two decades, an increasing number of studies has been devoted to a deeper understanding of the molecular process involved in the binding of various agonists and antagonists to active and inactive conformations of β_2-adrenergic receptor (β_2AR). The 3.2 Å x-ray crystal structure of human β_2AR active state in combination with the endogenous low affinity agonist adrenaline offers an ideal starting structure for studying the binding of various catecholamines to adrenergic receptors. We show that molecular docking of levodopa (L-DOPA) and droxidopa into rigid and flexible β_2AR models leads for both ligands to binding anchor sites comparable to those experimentally reported for adrenaline, namely D113/N312 and S203/S204/S207 side chains. Both ligands have a hydrogen bond network that is extremely similar to those of noradrenaline and dopamine. Interestingly, redocking neutral and protonated versions of adrenaline to rigid and flexible β_2AR models results in binding poses that are more energetically stable and distinct from the x-ray crystal structure. Similarly, lowest energy conformations of noradrenaline and dopamine generated by docking into flexible β_2AR models had binding free energies lower than those of best poses in rigid receptor models. Furthermore, our findings show that L-DOPA and droxidopa molecules have binding affinities comparable to those predicted for adrenaline, noradrenaline, and dopamine, which are consistent with previous experimental and computational findings and supported by the molecular dynamics simulations of β_2AR-ligand complexes performed here.

SIGNIFICANCE The β_2-adrenergic receptor, which belongs to the vast family of guanine nucleotide-binding protein coupled receptors, is a transmembrane protein that is activated by the catecholamines norepinephrine (noradrenaline) and epinephrine (adrenaline). Using molecular docking methods, we discovered that the exogenous ligands L-DOPA and droxidopa have the same hydrogen bond binding sites as endogenous agonists, such as adrenaline, noradrenaline, and dopamine. Furthermore, all of the catecholamines studied had different hydrophobic binding sites in the receptor. Our findings might help researchers to better understand how existing and new drugs chemically similar to droxidopa, which is used to treat Parkinson's disease, interact with β_2-adrenergic receptor.

INTRODUCTION

Guanine nucleotide-binding protein coupled receptors (GPCRs) are the most diverse family of human cell surface proteins, with over 800 members that play critical roles in biological functions, such as vision, sensing, and neurotransmission (1–3). GPCRs have also been identified to play an active role in cognitive responses (4), cardiovascular functions (5), and cancer growth and development (6). Given their implication in different human diseases, GPCRs have been the target of 35% of all marketed pharmacological medicines in the United States and globally (7–9). All GPCRs share the same structural architecture of seven transmembrane α-helices (TM-I–TM-VII), which are connected by extracellular (ECL1–ECL3) and intracellular (ICL1–ICL3) loops (10,11). Numerous extracellular molecules, including hormones and drugs, can activate and inactivate GPCRs acting as agonists and antagonists (blockers), respectively, with the former often causing conformational changes linked with specific protein activities (12). Furthermore, GPCRs are being viewed as allosteric machinery that can be triggered by ions, lipids, cholesterol, and water (13,14). During the last two decades, because of technological advances in crystallization methods, x-ray crystal structures of GPCRs have been released at an exponential pace (3,15). More than 150 GPCR structures have been co-crystallized with ligands and published in the Protein Data Bank (PDB) (16). Concurrently, a growing number of homology models has contributed to covering more than 10% of the

Submitted August 30, 2021, and accepted for publication November 3, 2021.
*Correspondence: andrea.catte@sns.it or vincenzo.barone@sns.it
Akash Deep Biswas and Andrea Catte contributed equally to this work.
Editor: Alan Grossfield.
https://doi.org/10.1016/j.bpj.2021.11.007

GPCR superfamily. Because understanding receptor-drug interactions at an atomic level is crtitical in structure-based drug discovery, molecular docking and molecular dynamics (MD) simulations have become popular tools for assisting drug design by revealing binding affinity, reaction mechanism, and protein-ligand interactions (17–22).

The β_2-adrenergic receptor (β_2AR), a class A GPCR expressed in pulmonary and cardiac myocyte tissues, is activated by hormones such as adrenaline and noradrenaline. The determination of the first high-resolution crystal structures of β_2AR bound to an inverse agonist (−)-carazolol (PDB: 2RH1) (23,24) and the antagonist (−)-timolol (PDB: 3D4S) (25), respectively, has contributed to shed some light on the inactive state of adrenergic receptors. Moreover, the first agonist-bound active-state x-ray crystal structures have also been resolved for β_2AR stabilized by a nanobody and a nucleotide-free Gs protein heterotrimer (26,27). In particular, the x-ray crystal structure of β_2AR in complex with the low affinity agonist adrenaline published by Ring et al. in 2013 (PDB: 4LDO) (28) has provided a structural template for studying the binding conformations and affinities of different agonists and antagonists. Based on fluorescence spectroscopy studies, catecholamines can induce different conformational changes in the β_2AR, involving the formation of multiple intermediate states of the adrenergic receptor (29–32). More recently, NMR spectroscopy experiments have verified the β_2AR's conformational heterogeneity, which is characterized by the coexistence of active, intermediate, and inactive states of the receptor (33). According to the database with the largest collection of GPCRs structures and mutants (www.gpcrdb.org), there are structures of human β_2AR in complex with 1365 ligands, 75 of them being drugs (7). Among these drugs interacting with $\beta_2$2AR, droxidopa (L-DOPS) is a L-serine substituted at the β-position by a 3,4-dihydroxyphenyl group (34). L-DOPS is likewise a cathecol and a L-tyrosine derivative, and its structure is identical to that of the non-natural amino acid L-DOPA. Droxidopa is a precursor of noradrenaline that is used in the treatment of neurogenic orthostatic hypotension and Parkinson's disease. Droxidopa is authorized in Japan and is now being studied in clinical studies in the United States, Canada, Australia, and Europe.

The results of the molecular docking of L-DOPA and droxidopa to the human β_2AR x-ray crystal structure released by Ring et al. in 2013 (PDB: 4LDO) (28) and their comparison with observations from representative full agonists, such as adrenaline and noradrenaline, as well as the partial agonist dopamine, are presented here. Each fully flexible ligand was docked into the β_2AR binding pocket using two different approaches: 1) a rigid receptor model derived from the PDB coordinates of the β_2AR x-ray crystal structure (PDB: 4LDO) and 2) a β_2AR receptor with flexible side chains of specific amino acids of its active binding site.

Molecular interactions between β_2AR and the aforementioned five ligands have been studied by combining MD simulations, binding free energy (BFE), and free energy landscape (FEL) calculations.

MATERIALS AND METHODS

β_2AR all-atom model preparation

The x-ray crystal structure of human β_2AR protein in the active-state conformation (PDB: 4LDO) was used to build up an all-atom model of its monomeric transmembrane domain form (28). Amino acids missing in the crystal structure, namely residues 1–28 and 343–413, were omitted (35). Intracellular residues 232–262 belonging to the ICL3 domain of the receptor, which were previously omitted or modeled (35,36), were modeled using a homology model of β_2AR generated by the Sali laboratory in 2008 (37) employing 2RH1 as a template and reported in the ModBase database of comparative protein structure models (Fig. 1 *A*). 2RH1 has 90% sequence identity with 4LDO and shows root mean-square deviation of 2.5 Å with 4LDO (residues 29–231 and 263–342) along the Cα backbone. T4L and Nb6B9 residues were deleted, and chain termini were capped with neutral groups (acetyl and methylamino) as previously reported in the literature (35,36,38,39). Water molecules and adrenaline ligand were also removed from the model. Four engineered mutations (M96T, M98T, N187E, and C265A) were mutated to reproduce the sequence of human β_2AR (28). All Lys and Arg residues were protonated. All Asp, Glu, and His (HSD) residues were deprotonated except Glu122 (GLH), Asp130 (ASH), and His172 (HSP), as previously reported (36,38). Because the β_2AR model is in the active state, Asp79 was left deprotonated because it has been suggested to reach the protonation state upon activation (40,41). Two disulfide bonds were also added to the β_2AR model by removing hydrogens bound to SG atoms in cysteine residues; they are located in ECL2 (Cys184–Cys190) and TM-III (Cys106–Cys191), and the latter contributes to the stabilization of ECL2 (42). The molecular modeling was performed using Visual Molecular Dynamics (VMD) 1.9.4, and the final structure of the β_2AR model was generated with the VMD psfgen plugin (43).

Molecular docking

We parameterized the force fields of L-DOPA (DAH) and droxidopa (see Supporting materials and methods, section A.1 for details of parameterization methodology) and performed 20-ns MD simulations of both ligands in water. The stable structure obtained from the MD simulations of DAH and DRO molecules were further aligned to adrenaline (ALE) obtained from the β_2AR x-ray crystal structure (PDB: 4LDO) to improve the choice of the search space (docking grid box) around the binding site of the receptor. The modified β_2AR model shown in Fig. 1 *A* was used as a rigid receptor. The residues D113, V117, T118, F193, T195, S203, S204, S207, N293, H296, N301, Y308, N312, and Y316 reported to form H-bonds with adrenaline (28) are kept as flexible for flexible docking simulations, which is in analogy with a previous study of dopamine in the D_2DR receptor (44).

In the case of L-DOPA, H296 and N301 were not included in the list of flexible residues because of the limitations of AutoDock Tools 1.5.6 the graphical user interface of AutoDock 4.2.6 (AD4) (45), whereas for droxidopa, H296, N301, and V117 were excluded by the list of flexible residues because this ligand has an additional torsional degree of freedom as compared with L-DOPA. For both receptor models, the docking box grid dimensions were 50 Å each for the *x*, *y*, and *z* axes, respectively, in the active site region with a resolution of 0.375 Å. The grid box size was 18.75 Å, which is more than 2.9 times the radius of gyration of both L-DOPA (2.77 Å) and droxidopa (2.91 Å) molecules, as recommended in (46). Nonpolar hydrogen atoms were merged to heavy atoms, and Gasteiger charges were assigned to each molecule. All torsions of the ligands and flexible residues were allowed to rotate during docking. 400 poses were generated using a maximal number of generations and energy evaluation of 27,000 and $5 \cdot \times 10^7$, respectively, for both rigid and flexible

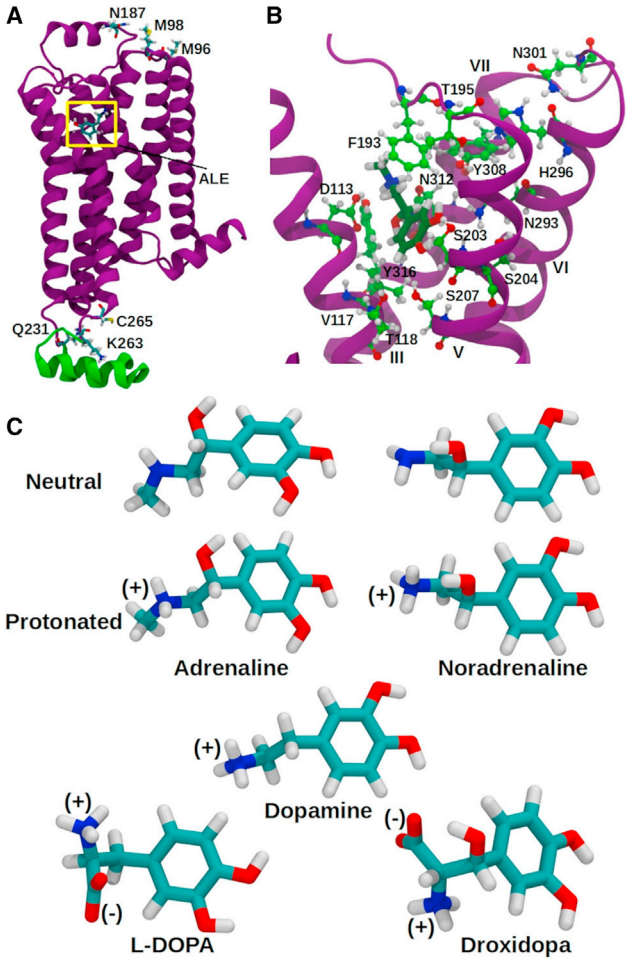

FIGURE 1 (*A*) A side view of the β_2AR model shows the main changes applied to 4LDO original structure with adrenaline (ALE) in its crystallographic binding site highlighted by a yellow square. β_2AR TM α-helices and the ICL3 domain are in purple and green, respectively. M96, M98, N187, and C265 residues, which are mutated in the x-ray crystal structure, and Q231 and K263 residues connecting 4LDO to the ICL3 domain are shown in licorice representation. (*B*) β_2AR residues of the binding pocket interacting with crystallographic adrenaline (*dark green*) are shown in green. TM α-helices III, V, VI, and VII are displayed in purple. (*C*) Chemical structures of neutral, protonated, and zwitterionic ligands employed in molecular dockings into rigid and flexible β_2AR models.

β_2AR models, as previously reported for the molecular docking of dopamine to the D_2DR receptor (44). Molecular docking of each ligand to rigid and flexible β_2AR models was also carried out employing the AutoDock Vina (Vina) package (47). Global search exhaustiveness of 400 (Nguyen et al. 2020 (48)) and a maximal energy-δ of 7 kcal/mol were used in each Vina run. Vina docking calculations were performed on each system using the same center and size of the grid generated with Autogrid4 for AD4 runs. The pythonsh command of AD4 was employed to perform the Virtual Screening analysis of final docked conformations, which were clustered using a tolerance of 2 Å root mean-square deviations (49,50). The structure with the highest binding affinity was selected as the best conformation of the ligand. After selecting the best conformations, 10 independent molecular docking calculations have also been performed for each ligand, mentioned further in the article.

The binding affinities of each ligand were calculated from the free energy of binding (ΔG_{bind} = -RTlnK_i) and inhibition constants (K_i) estimated by AutoDock for lowest energy structures (49). Binding free energies were converted to binding affinities ($pK_d = -\log 10\ K_d$) by the inhibition constant equation ($K_i = K_d = 10^{(\Delta G_{bind}/1.366)}$) (51).

This protocol was validated by redocking neutral and protonated adrenaline to the β_2AR x-ray crystal structure (PDB: 4LDO) (see Figs. S1–S8 for the results of both protonation states and Fig. 1 *C* for neutral forms) (52).

Hydrogen bond and hydrophobic contacts between each ligand and both models of the receptor were estimated using the protein-ligand interaction profiler (53). Images were prepared using VMD 1.9.4, AutoDock tools 1.5.6, and LigPlot + version 2.2 (54)

MD simulations of β_2AR-catecholamine complexes.

We performed all-atom MD simulations of β_2AR-catecholamine complexes embedded in hydrated lipid bilayers using the CHARMM36 force field (55–57) for 1 μs. Each of these simulations are available on the GPCRmd (22) database within the following links:

1) β_2AR-adrenaline, https://submission.gpcrmd.org/view/subid/366/;
2) β_2AR-noradrenaline, https://submission.gpcrmd.org/view/subid/367/;
3) β_2AR-dopamine, https://submission.gpcrmd.org/view/subid/369/;
4) β_2AR-L-DOPA, https://submission.gpcrmd.org/view/subid/368/; and
5) β_2AR-droxidopa https://submission.gpcrmd.org/view/subid/365/.

Further details are provided in the Supporting materials and methods, section A.8.

Essential dynamics and free energy landscape

Essential dynamics (ED) was used to analyze β_2AR-catecholamine complexes and extract larger amplitude motions observed in MD simulations. The protocol of ED calculations is described in the Supporting materials and methods, section A.9.

Binding free energy of ligands in β_2AR-catecholamine complexes

Binding free energies (BFEs) of ligands from MD simulations of β_2AR-catecholamine complexes were estimated using molecular mechanics Poisson-Boltzmann surface area (MM-PBSA) calculations (58). More details can be found in the Supporting materials and methods, section A.10.

RESULTS

Full and partial agonists binding to β_2AR: docking of noradrenaline and dopamine

To verify the quality of the β_2AR x-ray crystal structure (PDB: 4LDO) for the generation of biologically relevant ligand conformations, we redocked adrenaline to rigid and flexible receptor models following an approach similar to that of (59). Although adrenaline and noradrenaline (with pK_a of 8.52 and 8.75, respectively) are mostly present in their protonated forms (94.7%) at the physiological pH of 7.4, the population of neutral forms is not negligible (5.3%) (52). As a consequence, we performed the redocking using both forms (see Figs. S5–S8, S11–S14). The docking of protonated noradrenaline and dopamine into rigid β_2AR models produced for both ligands conformations similar to adrenaline (Fig. 2 *A*), confirming that they share the same

binding anchor sites (Fig. 2, *C–E*). Furthermore, structures with comparable conformations were generated by independent runs for both noradrenaline protonation states and dopamine (Figs. S13–S15). The binding free energies (BFEs) estimated from molecular docking to rigid models of the receptor for the lowest energy conformations of protonated noradrenaline and dopamine, −7.8 kcal/mol (Fig. S13) and −6.7 kcal/mol (Fig. S15), respectively, are comparable to those observed for adrenaline, implying that these low energy poses are also representative of thermodynamically stable poses.

In analogy with adrenaline (Fig. 2 *B*), docking of protonated noradrenaline and dopamine into flexible β_2AR models resulted in conformations structurally different from the best binding poses of the ligands in rigid models of the receptor (Fig. 2, *D–F*). Notably, both protonated noradrenaline and dopamine had highly favorable BFEs of −12.8 and −12.6 kcal/mol, respectively, which overestimated binding affinity values previously estimated by both experimental and computational approaches (Table 1) (59–61). Similar BFEs of endogenous ligands were calculated utilizing the MM-PBSA approach by analyzing MD simulations of β_2AR-catecholamine complexes (Table S5).

L-DOPA binding to the β_2AR receptor

The docking of L-DOPA into a rigid β_2AR model yielded 70% of the largest cluster conformations from 10 independent runs exhibiting an adrenaline-like interaction of the head and the tail of the catecholamine with S203/S204/S207 and D113/N312 anchor sites in the binding pocket (Fig. 3 *A*; Fig. S17; Table 3). These poses of the ligand showed an average BFE of −6.4 kcal/mol (Fig. S18) and a binding affinity of 4.7, close to the values observed for neutral adrenaline and dopamine (Table 1).

Docking of L-DOPA in the flexible β_2AR model provided more ligand-receptor hydrogen bond interactions as compared with the structure of the catecholamine generated by the docking into the rigid model of the receptor (Fig. 3 *B*; Table 3). The ligand's catechol head, in particular,

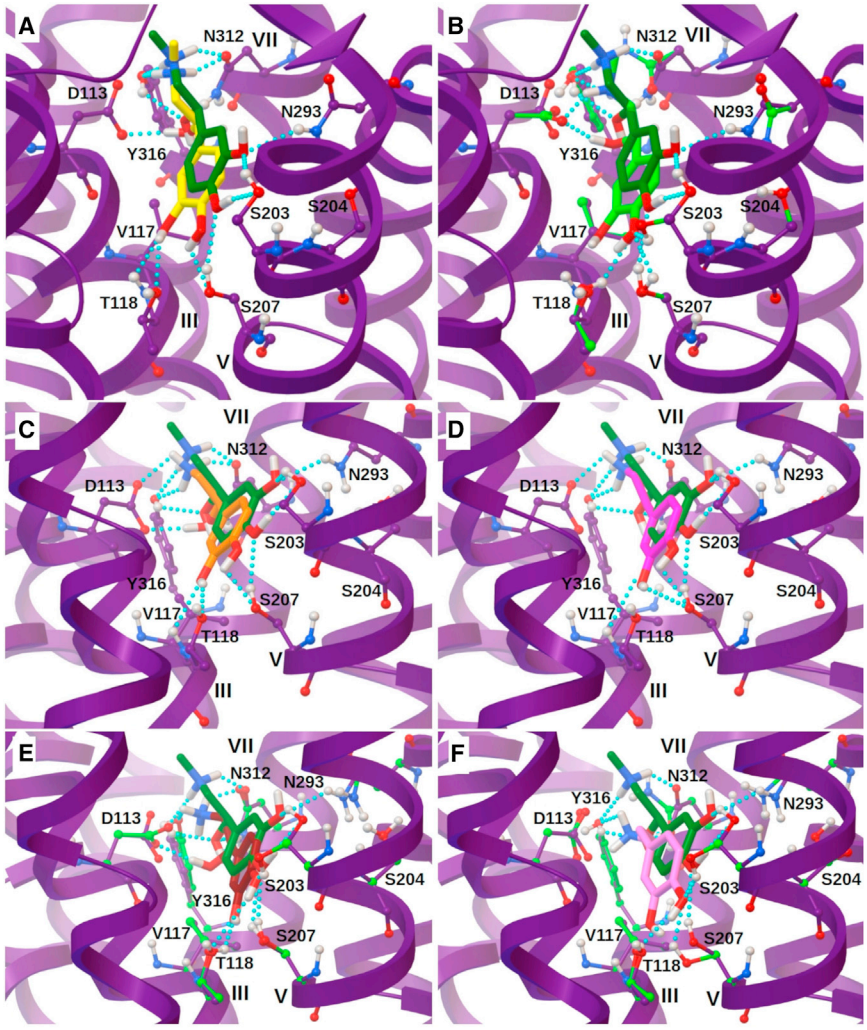

FIGURE 2 Lowest energy conformations of protonated adrenaline from one of the 10 independent runs of molecular docking into (*A*) rigid (*yellow*) and (*B*) flexible (*green*) β_2AR models are compared with the conformation of the ligand in the β_2AR x-ray crystal structure (PDB: 4LDO) (*dark green*). Lowest energy conformations from the molecular docking of protonated noradrenaline (*orange* and *brown*) and dopamine (*magenta* and *pink*) into (*C* and *D*) rigid and (*E* and *F*) flexible β_2AR models are compared with adrenaline's conformation in the x-ray crystal structure. The protein is shown as purple ribbons, and β_2AR side chains in contact with adrenaline are shown as sticks and balls. Carbon atoms of rigid and flexible side chains of β_2AR amino acid residues interacting with neutral adrenaline are shown in purple and green, respectively. Hydrogen bonds are shown with cyan spheres. All nonpolar hydrogens are not shown.

TABLE 1 Calculated binding affinities, pK_d, of different ligands for rigid and flexible β_2AR models obtained by AD4 and Vina calculations in comparison with experimental and MD simulations values

Ligand	Calculated binding affinity pK_d				Experimental binding affinity pK_d
	Rigid model[a]		Flexible model[a]		
	AD4	Vina	AD4	Vina	
Adrenaline (neutral)	4.6	5.5	6.1	5.6	6.1[b]–6.5[c] (11.7) [d]
Adrenaline (protonated)	5.9	5.5	9.2	5.6	
Noradrenaline (neutral)	5.6	5.3	9.0	5.3	5.0[b]–5.4[c] (5.3) [d]
Noradrenaline (protonated)	5.7	5.3	9.4	5.3	
Dopamine	4.9	5.1	9.2	5.3	3.8[b]– 4.1[c] (3.9)[d]
L-DOPA	4.7	5.3	9.4	5.8	(5.0)[d]
Droxidopa	5.4	5.5	10.3	5.8	(7.4)[d]

[a]Binding affinities calculated from binding free energies and averaged over 10 independent runs.
[b]Del Carmine et al. 2004 (61).
[c]Del Carmine et al. 2002 (60).
[d]pK_d values obtained by BFEs calculated from MD simulations are reported in parentheses (see Table S5).

established hydrogen bonds with the binding site amino acid T118. The average BFE of the lowest energy conformations was −12.8 kcal/mol (Fig S19), corresponding to a binding affinity of 9.4, which is close to values found for adrenaline, noradrenaline, and dopamine docked into flexible β_2AR models (Table 1). Furthermore, the BFE of the β_2AR-L-DOPA complex was equivalent to the experimental value of noradrenaline when calculated using the MM-PBSA method over a 1 μs MD simulation of 5.0 pK_d (Table 1).

Droxidopa binding to the β_2AR receptor

When docked to rigid β_2AR models, droxidopa exhibited conformations very similar to noradrenaline, adrenaline, and dopamine, in which the ligand's ethanolamine tail was anchored at the D113/N312 anchor site and its catechol head was bound only to S207 in TM-V (Fig. 3 *C*). The lowest energy conformation exhibited a BFE of −7.4 kcal/mol (Fig. S21) (average of best poses from 10 independent runs), which is very similar to noradrenaline (−7.6 kcal/mol), confirming our docking results. Furthermore, the binding affinities of droxidopa (5.4) and noradrenaline (5.6) were comparable and in line with experimental values available for the endogenous ligand (Table 1) (60,61).

Similarly to L-DOPA, the docking of droxidopa into the flexible β_2AR model resulted in optimal conformations displaying more hydrogen bond interactions with both anchor sites of the binding pocket of the receptor as compared with the ligand bound to the rigid model (Fig. 3 *D*). The lowest energy conformation of droxidopa in the flexible receptor model shows an average BFE of −14.0 kcal/mol (Fig. S22), which corresponds to a binding affinity of 10.3 (Table 1), and hydrogen bond interactions very similar to those observed in the best binding pose of the ligand in a rigid receptor model (Fig. 3 *C*). In particular, the hydrogen bond network of this structure is characterized by an additional interaction with N312 in the D113/N312 anchor site (Fig. 3 *D*; Table 3). Additionally, this conformation of droxidopa structures is most probably a representative pose of the ligand because it displays the characteristic and experimentally proven orientation of catecholamines in β_2AR models reported in this article and in the literature (Fig. S20) (59). As reported for the other exogenous ligand, the BFE of the β_2AR-droxidopa complex produced by employing the MM-PBSA method over a 1 μs MD simulation is −10.1 kcal/mol, which is in good agreement with the flexible docking result (Table S5).

Hydrogen bond network in β_2AR models bound to noradrenaline and dopamine

The best binding poses of protonated noradrenaline and dopamine in rigid β_2AR models showed hydrogen bond distances very similar to those observed for protonated adrenaline (Table 2, Fig. S13 and S15 and Supporting materials and methods, section A.5). Both anchor site amino acids D113 and N312 formed hydrogen bonds with the ethanolamine tail of each ligand, confirming both experimental and computational results (28,59,62). Moreover, hydrogen bond interactions were observed between the N312 side chain and the β-OH of noradrenaline, in good agreement with biochemical results (63). In the rigid receptor model, Y316 formed hydrogen bonds with the tail of each ligand as already observed for adrenaline and in agreement with the same interaction present in the x-ray crystal structure. Hydrogen bonds of catechol hydroxyls with side chains of serines of the TM-V helical domain, which are considered the most specific interactions for β_2AR agonists, were observed only between S207 and para-OH of each ligand (60,61,64–67). Hydrogen bonds involving T118 side chain and the catechol head moiety were also conserved for both endogenous ligands, suggesting that this amino acid contributes also to the network of H-bond interactions. Furthermore, the neutral form of noradrenaline displayed similar hydrogen bonds as observed for the protonated ligand (Table S1).

In analogy with both forms of adrenaline, the docking of protonated noradrenaline and dopamine into flexible β_2AR models resulted in a reduction in hydrogen bond distances for both ethanolamine tail and catechol head moieties of each ligand interacting with amino acid residues D113, Y316, and T118. Moreover, protonated noradrenaline also exhibited the two additional hydrogen bonds, as found in the case of adrenaline, between the catechol head hydroxyls and residues S203 and S207 (Table 2). In contrast, the catechol head of dopamine interacted differently with flexible

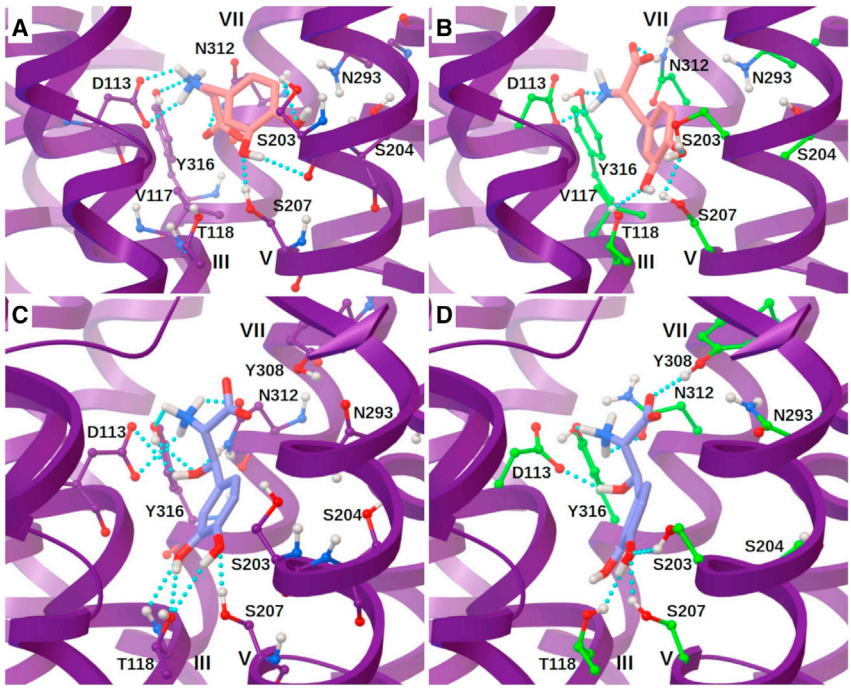

FIGURE 3 Conformations from the molecular docking of L-DOPA (*salmon*) and droxidopa (*violet*) to (*A* and *C*) rigid and (*B* and *D*) flexible β_2AR models. The largest cluster conformation of L-DOPA in a β_2AR rigid model forms more hydrogen bonds than the lowest energy conformation of the ligand in a flexible receptor. The lowest energy conformation of droxidopa in a β_2AR rigid model forms more hydrogen bonds than the lowest energy binding pose of the ligand in a flexible receptor. Color code and view point as in Fig. 2. Fig. S17 shows comparisons between lowest energy and largest cluster conformations of L-DOPA in β_2AR rigid models from 10 independent runs.

β_2AR serines forming only the hydrogen bond S207-meta-OH but still showing the strong S207-para-OH interaction observed in the rigid β_2AR model and previously reported in the literature (59). Similarly to adrenaline, the N293-meta-OH hydrogen bond found in the x-ray crystal structure of β_2AR (PDB: 4LDO) was not observed in all lowest energy conformations of noradrenaline and dopamine docked in rigid and flexible receptor models (28). This hydrogen bond interaction of the meta-OH of adrenaline with N293 has also been observed in β_2AR bound to the endogenous ligand in previous experimental works (66,68). The hydrogen bond with residue N293 was still not present in lowest energy binding poses of adrenaline, noradrenaline, and dopamine obtained by flexible docking AD4 runs using a shifted grid box center (Fig. S23). In particular, the lowest energy binding poses of noradrenaline and dopamine formed hydrogen bonds with T118, which have been previously observed through MD simulations of β_2AR bound to different ligands (69–73). Polar interactions with N293 were instead observed in all endogenous catecholamines subjected to flexible docking Vina runs (Fig. S23). To investigate this controversial docking result, we employed 1 μs β_2AR-catecholamines MD simulations. The hydrogen bonding of N293 with the catecholamine was established with a lifetime ranging from 4.1 to 22.7% over the whole simulation period, which is in good agreement with experimental results (see Table S4). In contrast with molecular docking findings, all endogenous catecholamines displayed very low percentages of hydrogen bond formation with T118, a consequence of the more pronounced formation of polar interactions with N293.

Hydrogen bond network in β_2AR models bound to L-DOPA and droxidopa

The hydrogen bond network of both L-DOPA and droxidopa docked in different β_2AR models exhibited some analogies, and remarkable differences as compared with that of endogenous catecholamines (Fig. 3; Table 3). In analogy with polar interactions observed for endogenous ligands, hydrogen bond distances decreased when using flexible receptor models (Table 3). Both ligands showed hydrogen bond interactions with residues D113 and N312 through their tail moieties. In the case of droxidopa, as observed for andrenaline and noradrenaline ligands, these polar interactions were strengthened by the presence of the β-OH group in the ethanolamine tail of the ligand, leading to the formation of H-bonds with D113 and N312 amino acids in both rigid and flexible β_2AR models (Table 3). However, in both receptor models, L-DOPA showed an additional interaction site by hydrogen bonding with N312 through one of its carboxyl oxygens. A similar hydrogen bond interaction was also observed in droxidopa docked in a flexible β_2AR model (Table 3). As observed for endogenous ligands (Table 2) and regardless of the receptor model employed, the N-amino of both ligands formed hydrogen bonds with Y316, which interacted with the β-OH group of droxidopa docked only in the rigid receptor model (Table 3).

In the rigid β_2AR model, the catechol head of L-DOPA formed hydrogen bonds with residues S203 and S207 through its para-OH and meta-OH hydroxyl groups, respectively (Table 3). This result is in contrast with experimental and computational results suggesting and predicting

TABLE 2 Hydrogen bond distances for different β_2AR-Ligand complexes from AD4 calculations

Hydrogen bonds (β_2AR-Ligand)	Donor-Acceptor distance (Å)					
	Rigid model			Flexible model		
	ALE	NLE	DOP	ALE	NLE	DOP
OD1 (D113)-N (amino)	**3.7** (**4.1**)[a]	**3.6**	3.5	2.8	2.8	2.2
OD2 (D113)-N (amino)	2.7 (2.8)	2.5	2.5	2.6	2.5	2.8
OD1 (D113)-O (β-OH)	3.0 (2.8)	2.8	–[b]	3.1	3.1	–
OG1 (T118)-O (para)	3.3 (**4.4**)	**3.6**	3.5	3.4	**3.6**	2.9
OG1 (T118)-O (meta)	3.2 (**7.0**)	3.3	3.0	2.6	2.8	2.7
OG (S203)-O (para)	**4.7** (**3.7**)	**4.3**	**4.2**	2.7	2.6	**4.7**
OG (S203)-O (meta)	**7.1** (3.2)	**7.1**	**7.0**	**5.1**	**6.3**	**7.2**
OG (S204)-O (para)	**6.5** (**5.7**)	**6.4**	**6.4**	**6.2**	**6.5**	**6.6**
OG (S204)-O (meta)	**8.7** (**4.8**)	**8.6**	**8.4**	**8.0**	**8.1**	**8.6**
OG (S207)-O (para)	2.6 (3.5)	2.8	2.8	3.1	2.9	2.0
OG (S207)-O (meta)	**4.0** (**6.0**)	**4.0**	**3.7**	2.8	3.2	3.5
OD1 (N312)-N (amino)	2.8 (2.8)	2.7	2.7	3.0	2.8	**3.7**
ND2 (N312)-O (β-OH)	2.9 (2.8)	2.8	–	**4.9**	3.3	–
OH (Y316)-N (amino)	3.4 (3.5)	3.0	3.0	3.3	2.6	2.7
OH (Y316)-O (β-OH)	**3.9** (3.5)	**3.7**	–	**4.1**	**4.2**	–

This analysis was performed on the following ligands: protonated adrenaline (ALE), protonated noradrenaline (NLE), and dopamine (DOP). Distances not compatible with hydrogen bonding are shown in bold characters.
[a]Hydrogen bonds of adrenaline's conformation in the β_2AR X-ray crystal structure (PDB: 4LDO) are shown in parentheses.
[b]-OH group is absent in the dopamine ligand.

TABLE 3 Hydrogen bond distances for different β_2AR-Ligand complexes from AD4 and Vina calculations

Hydrogen bonds (β_2AR-Ligand)	Donor-Acceptor distance (Å)			
	Rigid model		Flexible model	
	DAH	DRO	DAH	DRO
OD1 (D113)-N (amino)	3.0 (**4.0**)[a]	3.4 (**3.9**)	2.8 (**4.5**)	2.8 (**4.5**)
OD2 (D113)-N (amino)	2.5 (3.2)	2.4 (3.2)	2.5 (3.0)	2.3 (2.9)
OD1 (D113)-O (β-OH)	–[b]	2.7 (3.1)	–	2.9 (**3.6**)
OG1 (T118)-O (para)	**6.2** (**4.3**)	**3.6** (**4.0**)	3.1 (**4.4**)	3.1 (**4.0**)
OG1 (T118)-O (meta)	**3.7** (2.9)	3.3 (**6.8**)	2.7 (2.9)	3.1 (**6.9**)
OG (S203)-O (para)	2.8 (**3.7**)	**4.3** (**4.3**)	2.6 (**3.6**)	**4.7** (**3.9**)
OG (S203)-O (meta)	**4.3** (**6.2**)	**7.1** (3.1)	**4.9** (**6.1**)	**7.5** (2.9)
OG (S204)-O (para)	3.5 (**5.2**)	**6.3** (**5.9**)	**5.5** (**5.2**)	**6.9** (**5.8**)
OG (S204)-O (meta)	**6.2** (**7.8**)	**8.7** (**4.4**)	**7.8** (**7.7**)	**8.8** (**4.1**)
OG (S207)-O (para)	**4.5** (**2.8**)	2.9 (3.0)	2.5 (2.8)	2.7 (2.9)
OG (S207)-O (meta)	2.9 (3.1)	**4.1** (**5.6**)	3.1 (3.3)	**3.9** (**5.4**)
OD1 (N312)-N (amino)	2.9 (**5.4**)	2.7 (**5.3**)	3.0 (**6.1**)	2.9 (**5.7**)
ND2 (N312)-O (β-OH)	–	2.8 (3.1)	–	3.0 (3.3)
ND2 (N312)-O1 (-COO^-)	2.7 (**4.6**)	**4.6** (**5.7**)	2.5 (3.2)	3.5 (2.9)
ND2 (N312)-O2 (-COO^-)	**4.0** (**4.9**)	**5.3** (**4.8**)	**4.0** (3.2)	**5.0** (3.3)
OH (Y316)-N (amino)	3.0 (**5.3**)	2.9 (**5.2**)	2.4 (**5.2**)	2.4 (**5.1**)
OH (Y316)-O (β-OH)	–	3.5 (3.5)	–	**3.9** (**3.7**)

This analysis was performed on the following ligands: L-DOPA (DAH) and droxidopa (DRO). Distances not compatible with hydrogen bonding are shown in bold characters.
[a]Hydrogen bond distances from Vina calculations are reported in parentheses.
[b]-OH group is absent in the L-DOPA ligand.

hydrogen bond interactions of meta-OH and para-OH hydroxyls of the catechol head moiety of different catecholamines with S203 and S207, respectively (59,65,67). Interestingly, when docked into a rigid β_2AR model, L-DOPA forms also hydrogen bonds with S204 through the para-OH of its catechol head, showing another polar interaction not supported by experimental and computational results (59,65,67). However, the docking of L-DOPA in a flexible β_2AR model generated lowest energy conformations displaying also the hydrogen bond interaction of the para-OH hydroxyl of the catechol head moiety with S207, as reported in experimental and computational studies (59,65,67) (Table 3). Additionally, in the flexible β_2AR model, as observed for endogenous catecholamines (Table 2), both hydroxyl groups of L-DOPA's catechol head formed hydrogen bonds with T118 (Table 3). In contrast with L-DOPA, droxidopa's catechol head formed hydrogen bonds only with residues S207 and T118 of β_2AR in both receptor models (Table 3). In particular, in the case of droxidopa, the S207-para-OH hydrogen bond was particularly stable in rigid and flexible β_2AR models. Moreover, both hydroxyl groups of droxidopa's catechol head displayed hydrogen bond interactions with T118 in the flexible receptor model (Table 3). The ability to form hydrogen bonds with T118 was also detected in MD simulations of the receptor bound to the exogenous ligands (Table S4).

Like endogenous catecholamines, both L-DOPA and droxidopa did not exhibit hydrogen bond interactions with N293 in flexible docking AD4 runs using different grid box centers (Fig. 3; Fig. S24, *A* and *C*). However, Vina flexible docking calculations showed the formation of the hydrogen bond with residue N293 of β_2AR in both exogenous ligands (Fig. S24, *B* and *D*). The absence of hydrogen bonds with N293 was also confirmed by the low percentage of these polar interactions observed in MD simulations of β_2AR-catecholamine complexes (Table S4). However, interestingly, both exogenous ligands exhibited polar interactions with T118 with lifetimes comparable to those with N293, supporting molecular docking results (Table S4).

Hydrophobic contacts of β_2AR full and partial agonists

Similarly to adrenaline, AD4 and Vina lowest energy conformations of protonated noradrenaline formed hydrophobic contacts with V117 and F289 in rigid receptor models, in good agreement with a previous computational study (Fig. 4 *A*) (59). In flexible receptor models, protonated noradrenaline displayed the same hydrophobic interactions obtained by Vina calculations of the ligand docked in a rigid β_2AR model, whereas the AD4 approach led to the formation of more apolar contacts with residues V114 and V117 (Fig. 4 *A*). Regardless of the receptor model employed, neutral noradrenaline displayed hydrophobic interactions with the same amino acids observed for the protonated form of the ligand in both AD4 and Vina approaches. Similarly to protonated noradrenaline, the AD4 lowest energy

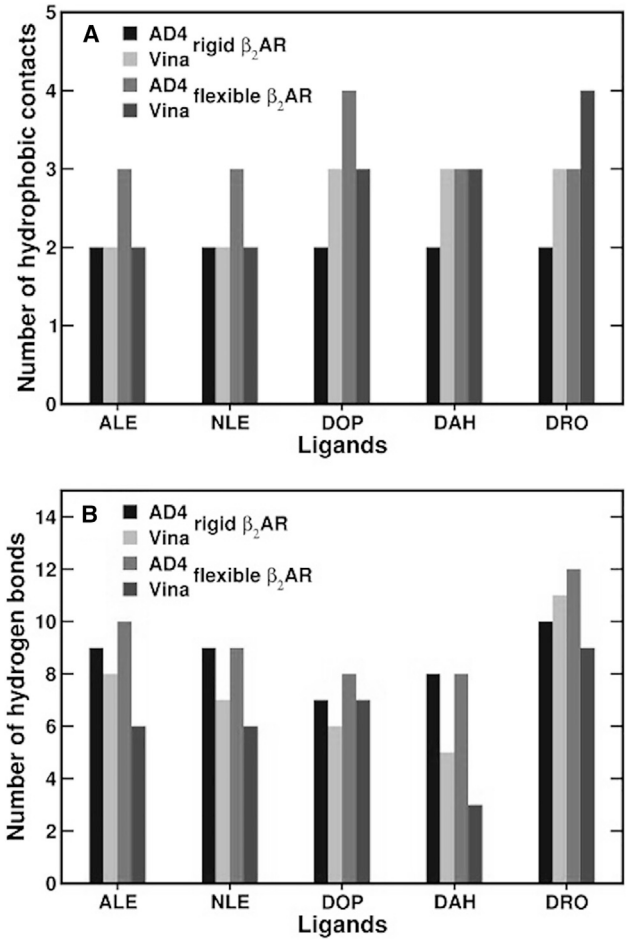

FIGURE 4 Number of (*A*) hydrophobic contacts and (*B*) hydrogen bonds between β_2AR amino acids and different catecholamines docked into rigid and flexible receptor models obtained by AD4 and Vina calculations. For clarity, only hydrophobic and hydrogen bond interactions of protonated adrenaline and noradrenaline are shown.

conformation of neutral noradrenaline interacted also with V114 and F290 (data not shown).

In rigid receptor models, both AD4 and Vina lowest energy conformations of dopamine interacted with β_2AR residues V117 and F289 as observed for adrenaline and protonated noradrenaline. The Vina lowest energy binding pose of the β_2AR partial agonist showed more hydrophobic contacts than the correspondent AD4 conformation, as a consequence of two F289 atoms interacting with the aromatic ring of dopamine (Fig. 4 *A*). When dopamine was docked into flexible β_2AR models, the AD4 approach led to more hydrophobic interactions than the Vina method. In particular, the AD4 best binding pose of dopamine formed hydrophobic contacts with V114 and V117 residues, as observed for protonated noradrenaline, whereas the Vina lowest energy conformation interacted with β_2AR amino acids V117, F193, and F289 (Fig. 4 *A*).

Interestingly, the precursor of dopamine L-DOPA displayed hydrophobic interactions with β_2AR residues V114 and F193, as shown by both AD4 and Vina calculations using rigid receptor models. Moreover, the Vina lowest energy binding pose of L-DOPA in a rigid β_2AR model showed also an additional hydrophobic contact with residue V117 (Fig. 4 *A*). Independently from the molecular docking software, the same number of hydrophobic interactions was observed when L-DOPA was docked into flexible β_2AR models (Fig. 4 *A*). AD4 lowest energy conformations of L-DOPA displayed apolar interactions with V117 and F289, whereas Vina binding poses showed hydrophobic contacts with the same amino acids of the rigid docking approach, namely V114, V117, and F193.

Similarly to protonated noradrenaline, in rigid β_2AR models, the AD4 lowest energy conformation of droxidopa interacted with residues V117 and F289, whereas the Vina best binding pose showed hydrophobic contacts with V114, V117, and F193, as observed with L-DOPA (Fig. 4 *A*). In flexible β_2AR models, droxidopa best binding poses obtained by the AD4 approach showed hydrophobic contacts with V114, V117, and F289, whereas the Vina lowest energy conformation displayed more apolar interactions with residues V114, F193, and F289 (Fig. 4 *A*; Fig. S25).

It is remarkable that the same apolar interactions with specific receptor residues, namely V114, V117, F193, A200, W286, F289, and F290, were also observed in MD simulations of β_2AR-catecholamine complexes as evidenced by the analysis of the percentage of hydrophobic contacts (Fig. S25).

ED and free energy landscape

To have an outline of the structural ensembles, we performed an ED analysis of the MD simulation trajectories of the β_2AR-catecholamines (binding affinities ranging from 4.6 to 10.3 pK_d, see Table 1). This analysis shows that the ensembles created by MD simulations covered a large portion of the configurational space (Fig. S26). Major conformations between a few distinct conformational states are assumed to be fairly well defined by projections onto the first two principal components seen in Fig. 5 (see two-dimensional (2D) MD Projections in Fig. S26). This demonstrates that the ensemble has a structural drift and falls approximately into various clusters of points, which provides the structural basis for the β_2AR-catecholamine structures. FEL simulations were performed specifically to confirm this behavior of the protein structure and to clarify the conformational variations of the clusters. The Gibbs free energy differences are seen in Fig. 5 (see also 2D and three-dimensional (3D) FEL in Fig. S26). It is remarkable that major deep free energy basins fall in the global free energy minimal region, meaning that stable conformational states exist within the well. In Fig. 5 (2D and 3D FEL), the lowest energy conformations are evidenced in blue.

DISCUSSION

In this work, we analyzed the binding of endogenous and exogenous catecholamines to the β_2AR adrenergic receptor

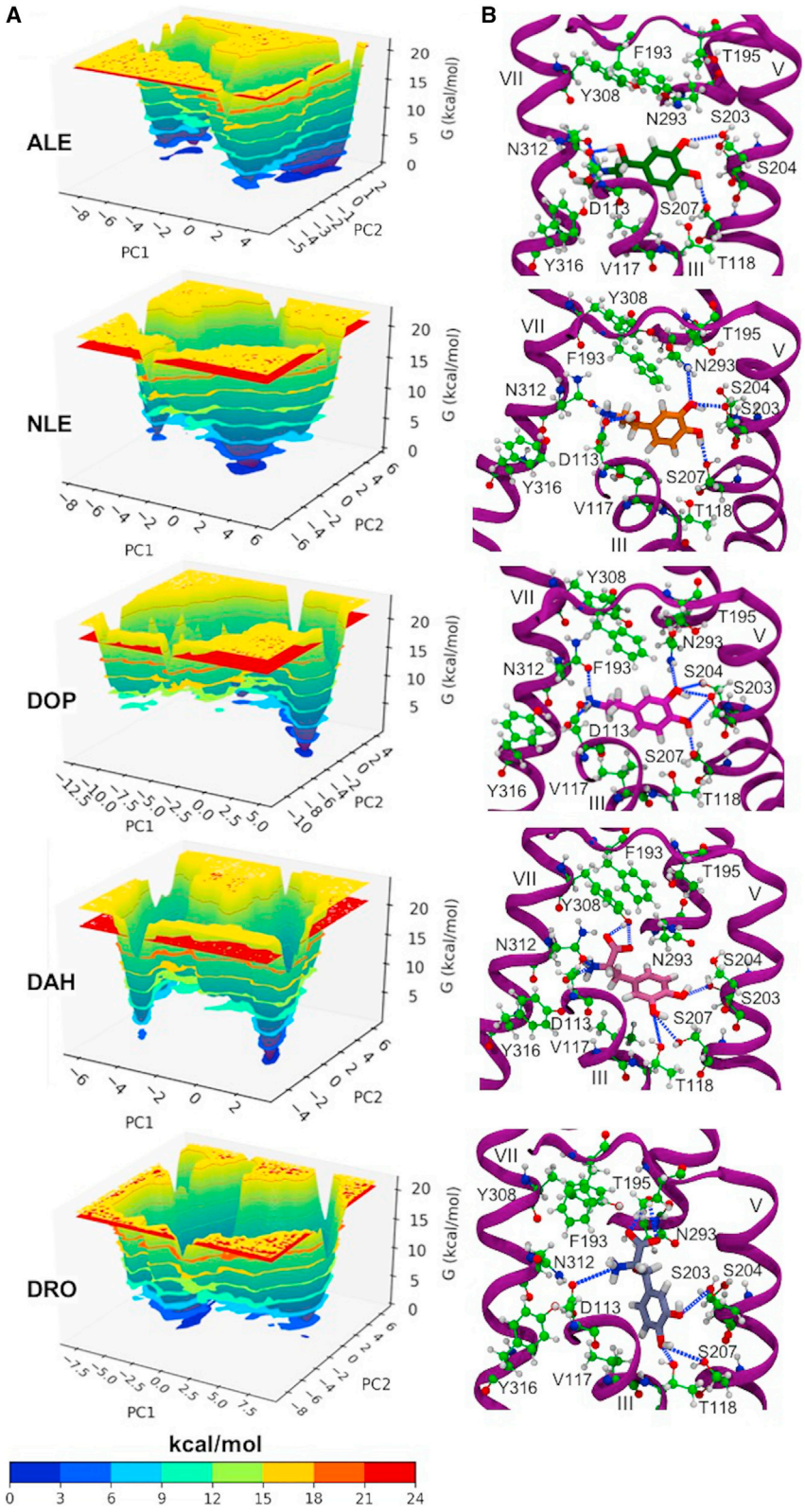

FIGURE 5 For a Figure360 author presentation of this figure, see https://doi.org/10.1016/j.bpj.2021.11.007 (*A*) 3D free energy landscapes derived from MD simulations of β_2AR complexes by projecting trajectories onto their own first (PC1) and second (PC2) eigenvectors. The energy scale, defined by the color bar in kcal/mol, ranges from blue to red, representing most and least stable structures, respectively. (*B*) Snapshots of MD simulations of β_2AR complexes show the hydrogen bond network of each ligand with specific amino acids of the receptor binding site. Hydrogen bonds are highlighted with dashed blue lines. Figure360▷

using molecular docking and MD simulations. Regardless of the β_2AR starting model, Vina calculations generated lowest energy poses of each catecholamine with binding affinities comparable to experimental results (Table 1) (48). Remarkably, in rigid docking simulations, the AD4 approach led to lowest energy conformations with BFEs

in good agreement with experimental values, whereas all ligands docked into flexible β_2AR models exhibited more than experimentally favorable binding affinities (48). These extremely favorable BFEs were also confirmed by MM-PBSA calculations performed on the MD trajectories of β_2AR-catecholamine complexes (Table S5). To the best of our knowledge, we have found novel lowest energy conformations of endogenous ligands, namely adrenaline, noradrenaline, and dopamine, docked into both rigid and flexible β_2AR models. These novel conformations are quite different from the structures predicted experimentally and computationally, suggesting that catecholamines interacting with adrenergic receptors can also adopt more energetically favorable binding modes (28,59). Interestingly, the lowest energy binding poses of exogenous ligands, namely L-DOPA and droxidopa, were similar to those observed for dopamine and noradrenaline, respectively, which are their closely related endogenous catecholamines (Figs. 2 and 3).

The presence of a different protonation state affected the binding affinity of adrenaline and noradrenaline to β_2AR, confirming that protonated forms of catecholamines are more stable than neutral ones (Table 1; Figs. S6, S7, S12, and S14) (52). In particular, BFEs of protonated adrenaline in the x-ray crystal structure and from the AD4 rigid docking approach corresponded to binding affinities of 5.2 and 5.9 (pK_d = 5.5 for Vina calculations), respectively, improving the 2.6 value measured by Katritch et al. in 2009 (59) for the rigid docking of the same ligand into a different β_2AR x-ray crystal structure (PDB: 2RH1) (Table 1) (23). The inclusion of some flexibility in the TM-V α-helical domain, which plays a critical role in the binding of full and partial agonists to β_2AR, allowed Katritch et al. in 2009 (59) to estimate for adrenaline a binding affinity of 5.7 (59), which is closer to the experimental pK_d values of 6.5 and 6.1 reported by Del Carmine et al. in 2002 and 2004, respectively (60,61). Our improved rigid docking pK_d values are most probably due to a different tilt of the TM-V domain in the two β_2AR x-ray crystal structures reported by Cherezov et al. in 2007 and Ring et al. in 2013 (23,28), suggesting its crucial role in inactive and active states of the adrenergic receptor. Moreover, our results confirm Katritch et al.'s (59) predictions on the importance of TM-V tilting in bringing the two anchor sites of the binding pocket, namely S203/S204/S207 and D113/N312, at a distance required to provide simultaneous hydrogen bond interactions with both head and tail groups of catecholamines (15,59).

Interestingly, the introduction of flexibility in residues belonging to the β_2AR binding pocket generated even more stable conformations for each studied ligand. As a consequence of the larger explored conformational space, the AD4 approach allowed all catecholamines to adopt binding poses with estimated binding free energies much lower than correspondent experimental and rigid docking values (59–61). In particular, the binding affinity of L-DOPA and droxidopa almost doubled for both ligands docked into flexible β_2AR models as compared with rigid receptor models (Table 1).

Our observations on the hydrogen bond network of each investigated catecholamine characterized the important role of key amino acids, such as D113, N312, S203, and S207, still acting as anchor sites for the formation of hydrogen bonds, in the binding of endogenous and exogenous catecholamines to both rigid and flexible β_2AR models generated from the x-ray crystal structure of the adrenergic receptor bound to the full agonist adrenaline (PDB: 4LDO) (Table 2 and 3) (28). The amino acid residue of TM-III, D113, has been found to be involved in the stabilization of β_2AR in complex with agonists (26). The crucial role for agonist binding to β_2AR played by S203 and S207 residues of TM-V is also supported by mutagenesis studies (60,65,66). Moreover, all these polar interactions of β_2AR residues with agonists are also considered to be important for the conformational stability of a region of the receptor containing TM-III, TM-IV, and TM-V α-helical domains, as shown by atomic force microscopy-based single-molecule force spectroscopy experiments (74). As highlighted mainly by AD4 calculations, we also found that Y316 residue of β_2AR TM-VII α-helical domain formed hydrogen bonds with the N of the amino group of the ethanolamine moiety of each studied ligand, contributing to the stability of lowest energy conformations of catecholamines. Both AD4 and Vina approaches showed that the β_2AR TM-III α-helical domain formed hydrogen bonds with the catechol head of each ligand through the amino acid T118, in good agreement with recent MD simulations results (69–73), evidence of which has also been found through our MD simulations results for the exogenous ligands (see Table S4). We also observed that the TM-VI residue N293 did not form hydrogen bonds with the catechol head of each tested ligand, which are stabilizing polar interactions for catecholamines bound to β_2AR (28,66,68). Interestingly, this experimentally supported hydrogen bond was successfully reproduced by slightly shifting the grid box center toward the N293 amino acid of β_2AR in Vina calculations of all catecholamines docked into flexible receptor models (Fig. S23, *B*, *D*, and *F*; Fig. S24, *B* and *D*). More interestingly, lowest energy conformations of all investigated catecholamines obtained by AD4 calculations of these ligands docked into flexible β_2AR models using a shifted grid box center did not display the hydrogen bond interaction between residue N293 and the catechol head moiety (Fig. S23, *A*, *C*, and *E*; Fig. S24, *A* and *C*). Moreover, the best binding poses of these ligands were both structurally and energetically similar to those observed with the original grid box center, indicating that these conformations could be novel binding modes of catecholamines to β_2AR. This difference in the hydrogen bond network is most probably due to the much smaller ensemble of ligands conformations sampled by Vina calculations, which on average generated a maximum of 20 best binding poses as compared with the

400 ligand conformations produced by the AD4 approach. To investigate further the aforementioned discrepancies, we used 1 μs MD simulations of the β_2AR-catecholamines and obtained evidence that N293 may also form hydrogen bonds. The N293 H-bond may be formed from 4.1% for ALE to 22.7% for DOP during the 1 μs MD simulation (Table S4). In exogenous ligands, we have observed the formation of both N293 and T118 H-bonds, the latter with lifetimes ranging from 3.4% for L-DOPA to 18.9% for droxidopa (Table S4).

The aromatic ring of investigated catecholamines can potentially interact with different β_2AR hydrophobic residues, such as V114, V117, F193, Y199, W286, F289, and F290 as reported for the x-ray crystal structure of β_2AR bound to carazolol (PDB: 2RH1) and various ligands studied computationally (23,59). In the β_2AR x-ray crystal structure released by Ring et al. in 2013 (PDB: 4LDO) (28), protonated adrenaline shows five hydrophobic contacts with V114, V117, F193, and F289 residues because two atoms of V117 interact with the catechol head of the natural ligand. In our case, AD4 and Vina approaches gave the same number of hydrophobic contacts, mainly with V117 and F289 residues, for lowest energy conformations of protonated adrenaline and noradrenaline docked into rigid β_2AR models (Fig. 4 *A*). At the same time, Vina best binding poses of dopamine, L-DOPA, and droxidopa interacting with rigid receptor models displayed an additional hydrophobic interaction as compared with the correspondent AD4 lowest energy structures (Fig. 4 *A*). In particular, the exogenous ligands, L-DOPA and droxidopa, displayed apolar interactions with V114 and F193, which are considered key residues in the binding of catecholamines to β_2AR (Fig. 4 *A*). In general, in AD4 rather than in Vina calculations of endogenous ligands docked into flexible β_2AR models, we also observed more hydrophobic contacts because of interactions with residues V114 and F290 (Fig. 4 *A*). AD4 lowest energy conformations of L-DOPA and droxidopa docked into flexible β_2AR models showed hydrophobic interactions mainly with V114, V117, and F289 residues (Fig. 4 *A*). Vina best binding poses of exogenous ligands displayed the same interactions observed by the AD4 approach and an additional interaction with F193 residue of β_2AR (Fig. 4 *A*). Taken together, the results of apolar interactions showed that all investigated catecholamines formed hydrophobic contacts with five out of seven β_2AR residues, namely V114, V117, F193, F289, and F290, as previously reported in the literature (59). It is also worth noting that all MD simulations of β_2AR-catecholamine complexes displayed the formation of hydrophobic interactions with the same amino acids obtained by AD4 and Vina calculations (Fig. S25).

Among all investigated catecholamines, the number of hydrophobic contacts was on average much lower than the number of hydrogen bonds with β_2AR residues and essentially constant for AD4 calculations, suggesting that polar interactions contribute more than apolar ones to all estimated binding free energies and affinities (Fig. 4 *B*). In particular, this difference between protein-ligand interactions became more evident in flexible dockings, thus explaining why AD4 calculations generated conformations with a higher binding affinity than those obtained by the Vina approach (Fig. 4 *B*; Tables S3 and S4).

CONCLUSIONS

Here, we hypothesize through molecular docking and MD simulations that the binding of catecholamines to β_2AR is stabilized by polar interactions of their catechol and ethanolamine moieties with specific amino acids, such as S203, S204, S207, D113, and N312, as observed by experimental and computational studies (59–61,64,67). We also showed that the network of polar interactions includes hydrogen bonds between Y316 and T118 residues of β_2AR and catechol head and ethanolamine tail atoms, respectively, contributing to the stability of lowest energy binding conformations of each ligand. In addition, each investigated catecholamine made also hydrophobic contacts with β_2AR residues, comprising V114, V117, F193, F289, and F290, previously observed to interact with similar agonists (59). The combination of AD4 and Vina approaches enabled us to explore in a more detailed way the conformational space of each ligand docked into flexible β_2AR models, leading to the discovery of novel binding modes for endogenous catecholamines. The exogenous catecholamines, L-DOPA and droxidopa, showed lowest energy binding conformations similar to their endogenous derivatives, dopamine and noradrenaline, respectively. At the same time, our study highlighted for the first time, to our knowledge, how the droxidopa drug interacts with β_2AR, suggesting similar binding modes for other structurally similar drugs employed in the treatment of Parkinson's disease. Despite the fact that these novel conformations of both endogenous and exogenous catecholamines are not yet validated experimentally, the structural variability of β_2AR active states should be considered. It is reasonable to expect that these novel binding modes would be possible under physiological conditions as well (74).

Besides, because excess levels of adrenaline and noradrenaline are implicated in cancer growth and development (75), a better understanding of how these hormones bind to β_2AR and other adrenergic receptors in healthy and tumoral cells might provide insight on the prevalence of these various binding modes.

SUPPORTING MATERIAL

Supporting material can be found online at https://doi.org/10.1016/j.bpj.2021.11.007.

AUTHOR CONTRIBUTIONS

A.C. and V.B. conceived the project. G.M. and V.B. jointly supervised this work. A.C. performed quantum mechanical calculations and force field parameterization, A.D.B. and A.C. performed the MD simulations of L-DOPA and droxidopa under the supervision of G.M., and A.D.B. and A.C. carried out Vina and AD4 molecular docking simulations, respectively. A.D.B. and A.C. analyzed the data and wrote the manuscript. All authors read and approved the final manuscript.

ACKNOWLEDGMENTS

Authors acknowledge Dr. Sara Del Galdo for her contribution in the performance of quantum mechanical calculations, force field parameterization, and MD simulations of L-DOPA and droxidopa ligands. We thank the SMART SNS Laboratory for high-performance computing resources and Alberto Coduti for providing assistance with software installation and managing.

A.D.B., A.C., G.M., and V.B. acknowledge the "Ministero dell'Istruzione, dell'Universita' e della Ricerca" PRIN 2017 (grant 2017A4XRCA) and by the Italian Space Agency (ASI; "Life in Space" project, N. 2019-3-U.0).

REFERENCES

1. Lee, Y., R. Lazim, …, S. Choi. 2019. Importance of protein dynamics in the structure-based drug discovery of class A G protein-coupled receptors (GPCRs). *Curr. Opin. Struct. Biol.* 55:147–153.
2. Latorraca, N. R., A. J. Venkatakrishnan, and R. O. Dror. 2017. GPCR dynamics: structures in motion. *Chem. Rev.* 117:139–155.
3. Gacasan, S. B., D. L. Baker, and A. L. Parrill. 2017. G protein-coupled receptors: the evolution of structural insight. *AIMS Biophys.* 4:491–527.
4. Chien, E. Y. T., W. Liu, …, R. C. Stevens. 2010. Structure of the human dopamine D3 receptor in complex with a D2/D3 selective antagonist. *Science.* 330:1091–1095.
5. Yang, J., V. A. M. Villar, …, C. Zeng. 2016. G protein-coupled receptor kinases: crucial regulators of blood pressure. *J. Am. Heart Assoc.* 5:1–13.
6. Bar-Shavit, R., M. Maoz, …, B. Uziely. 2016. G protein-coupled receptors in cancer. *Int. J. Mol. Sci.* 17:1320–1325.
7. Hauser, A. S., M. M. Attwood, …, D. E. Gloriam. 2017. Trends in GPCR drug discovery: new agents, targets and indications. *Nat. Rev. Drug Discov.* 16:829–842.
8. Hauser, A. S., S. Chavali, …, M. M. Babu. 2018. Pharmacogenomics of GPCR drug targets. *Cell.* 172:41–54.e19.
9. Sriram, K., and P. A. Insel. 2018. G protein-coupled receptors as targets for approved drugs: how many targets and how many drugs? *Mol. Pharmacol.* 93:251–258.
10. Fredriksson, R., M. C. Lagerström, …, H. B. Schiöth. 2003. The G-protein-coupled receptors in the human genome form five main families. Phylogenetic analysis, paralogon groups, and fingerprints. *Mol. Pharmacol.* 63:1256–1272.
11. Pierce, K. L., R. T. Premont, and R. J. Lefkowitz. 2002. Seven-transmembrane receptors. *Nat. Rev. Mol. Cell Biol.* 3:639–650.
12. Tyndall, J. D. A., and R. Sandilya. 2005. GPCR agonists and antagonists in the clinic. *Med. Chem.* 1:405–421.
13. Chattopadhyay, A. 2014. GPCRs: lipid-dependent membrane receptors that act as drug targets. *Adv. Biol.* 2014:e143023.
14. Chattopadhyay, A., and Y. D. Paila. 2007. Lipid-protein interactions, regulation and dysfunction of brain cholesterol. *Biochem. Biophys. Res. Commun.* 354:627–633.
15. Katritch, V., V. Cherezov, and R. C. Stevens. 2013. Structure-function of the G protein-coupled receptor superfamily. *Annu. Rev. Pharmacol. Toxicol.* 53:531–556.
16. Berman, H. M., J. Westbrook, …, P. E. Bourne. 2000. The protein data bank. *Nucleic Acids Res.* 28:235–242.
17. Nakliang, P., R. Lazim, …, S. Choi. 2020. Multiscale molecular modeling in G protein-coupled receptor (GPCR)-ligand studies. *Biomolecules.* 10:631.
18. Basith, S., M. Cui, …, S. Choi. 2018. Exploring G protein-coupled receptors (GPCRs) ligand space via cheminformatics approaches: impact on rational drug design. *Front. Pharmacol.* 9:128.
19. Heifetz, A., T. James, …, P. C. Biggin. 2016. Guiding lead optimization with GPCR structure modeling and molecular dynamics. *Curr. Opin. Pharmacol.* 30:14–21.
20. Yuan, X., and Y. Xu. 2018. Recent trends and applications of molecular modeling in GPCR-ligand recognition and structure-based drug design. *Int. J. Mol. Sci.* 19:2105.
21. Lee, Y., S. Basith, and S. Choi. 2018. Recent advances in structure-based drug design targeting class A G protein-coupled receptors utilizing crystal structures and computational simulations. *J. Med. Chem.* 61:1–46.
22. Rodríguez-Espigares, I., M. Torrens-Fontanals, …, J. Selent. 2020. GPCRmd uncovers the dynamics of the 3D-GPCRome. *Nat. Methods.* 17:777–787.
23. Cherezov, V., D. M. Rosenbaum, …, R. C. Stevens. 2007. High-resolution crystal structure of an engineered human beta2-adrenergic G protein-coupled receptor. *Science.* 318:1258–1265.
24. Rosenbaum, D. M., V. Cherezov, …, B. K. Kobilka. 2007. GPCR engineering yields high-resolution structural insights into beta2-adrenergic receptor function. *Science.* 318:1266–1273.
25. Hanson, M. A., V. Cherezov, …, R. C. Stevens. 2008. A specific cholesterol binding site is established by the 2.8 A structure of the human beta2-adrenergic receptor. *Structure.* 16:897–905.
26. Rasmussen, S. G. F., H.-J. Choi, …, B. K. Kobilka. 2011. Structure of a nanobody-stabilized active state of the β(2) adrenoceptor. *Nature.* 469:175–180.
27. Rasmussen, S. G. F., B. T. DeVree, …, B. K. Kobilka. 2011. Crystal structure of the β2 adrenergic receptor-Gs protein complex. *Nature.* 477:549–555.
28. Ring, A. M., A. Manglik, …, B. K. Kobilka. 2013. Adrenaline-activated structure of β2-adrenoceptor stabilized by an engineered nanobody. *Nature.* 502:575–579.
29. Swaminath, G., Y. Xiang, …, B. K. Kobilka. 2004. Sequential binding of agonists to the beta2 adrenoceptor. Kinetic evidence for intermediate conformational states. *J. Biol. Chem.* 279:686–691.
30. Swaminath, G., X. Deupi, …, B. Kobilka. 2005. Probing the beta2 adrenoceptor binding site with catechol reveals differences in binding and activation by agonists and partial agonists. *J. Biol. Chem.* 280:22165–22171.
31. Kobilka, B. K., and X. Deupi. 2007. Conformational complexity of G-protein-coupled receptors. *Trends Pharmacol. Sci.* 28:397–406.
32. Kobilka, B. 2013. The structural basis of G-protein-coupled receptor signaling (Nobel Lecture). *Angew. Chem. Int.Engl.* 52:6380–6388.
33. Nygaard, R., Y. Zou, …, B. K. Kobilka. 2013. The dynamic process of β(2)-adrenergic receptor activation. *Cell.* 152:532–542.
34. Katsube, J., H. Narabayashi, …, T. Suzuki. 1994. [Development of L-threo-DOPS, a norepinephrine precursor amino acid]. *Yakugaku Zasshi.* 114:823–846.
35. Rosenbaum, D. M., C. Zhang, …, B. K. Kobilka. 2011. Structure and function of an irreversible agonist-β(2) adrenoceptor complex. *Nature.* 469:236–240.
36. Dror, R. O., D. H. Arlow, …, D. E. Shaw. 2009. Identification of two distinct inactive conformations of the beta2-adrenergic receptor reconciles structural and biochemical observations. *Proc. Natl. Acad. Sci. USA.* 106:4689–4694.

37. Pieper, U., B. M. Webb, …, A. Sali. 2014. ModBase, a database of annotated comparative protein structure models and associated resources. *Nucleic Acids Res.* 42:D336–D346.

38. Dror, R. O., D. H. Arlow, …, D. E. Shaw. 2011. Activation mechanism of the β2-adrenergic receptor. *Proc. Natl. Acad. Sci. USA.* 108:18684–18689.

39. Dilcan, G., P. Doruker, and E. D. Akten. 2019. Ligand-binding affinity of alternative conformers of human β_2 -adrenergic receptor in the presence of intracellular loop 3 (ICL3) and their potential use in virtual screening studies. *Chem. Biol. Drug Des.* 93:883–899.

40. Vanni, S., M. Neri, …, U. Rothlisberger. 2010. A conserved protonation-induced switch can trigger "ionic-lock" formation in adrenergic receptors. *J. Mol. Biol.* 397:1339–1349.

41. Ranganathan, A., R. O. Dror, and J. Carlsson. 2014. Insights into the role of Asp79(2.50) in β2 adrenergic receptor activation from molecular dynamics simulations. *Biochemistry.* 53:7283–7296.

42. Bang, I., and H.-J. Choi. 2015. Structural features of β2 adrenergic receptor: crystal structures and beyond. *Mol. Cells.* 38:105–111.

43. Humphrey, W., A. Dalke, and K. Schulten. 1996. VMD: visual molecular dynamics. *J. Mol. Graph.* 14:33–38, 27–28..

44. Tosso, R. D., O. Parravicini, …, R. D. Enriz. 2020. Conformational and electronic study of dopamine interacting with the D_2 dopamine receptor. *J. Comput. Chem.* 41:1898–1911.

45. Morris, G. M., R. Huey, …, A. J. Olson. 2009. AutoDock4 and AutoDockTools4: automated docking with selective receptor flexibility. *J. Comput. Chem.* 30:2785–2791.

46. Feinstein, W. P., and M. Brylinski. 2015. Calculating an optimal box size for ligand docking and virtual screening against experimental and predicted binding pockets. *J. Cheminform.* 7:18.

47. Trott, O., and A. J. Olson. 2010. AutoDock Vina: improving the speed and accuracy of docking with a new scoring function, efficient optimization, and multithreading. *J. Comput. Chem.* 31:455–461.

48. Nguyen, N. T., T. H. Nguyen, …, S. T. Ngo. 2020. Autodock vina adopts more accurate binding poses but autodock4 forms better binding affinity. *J. Chem. Inf. Model.* 60:204–211.

49. Cosconati, S., S. Forli, …, A. J. Olson. 2010. Virtual screening with AutoDock: theory and practice. *Expert Opin. Drug Discov.* 5:597–607.

50. Cosconati, S., L. Marinelli, …, A. J. Olson. 2012. Protein flexibility in virtual screening: the BACE-1 case study. *J. Chem. Inf. Model.* 52:2697–2704.

51. Onawole, A. T., T. U. Kolapo, …, R. O. Adegoke. 2018. Structure based virtual screening of the Ebola virus trimeric glycoprotein using consensus scoring. *Comput. Biol. Chem.* 72:170–180.

52. Álvarez-Diduk, R., and A. Galano. 2015. Adrenaline and noradrenaline: protectors against oxidative stress or molecular targets? *J. Phys. Chem. B.* 119:3479–3491.

53. Salentin, S., S. Schreiber, …, M. Schroeder. 2015. PLIP: fully automated protein-ligand interaction profiler. *Nucleic Acids Res.* 43:W443-7.

54. Laskowski, R. A., and M. B. Swindells. 2011. LigPlot+: multiple ligand-protein interaction diagrams for drug discovery. *J. Chem. Inf. Model.* 51:2778–2786.

55. Klauda, J. B., R. M. Venable, …, R. W. Pastor. 2010. Update of the CHARMM all-atom additive force field for lipids: validation on six lipid types. *J. Phys. Chem. B.* 114:7830–7843.

56. Best, R. B., X. Zhu, …, A. D. Mackerell, Jr. 2012. Optimization of the additive CHARMM all-atom protein force field targeting improved sampling of the backbone ϕ, ψ and side-chain χ(1) and χ(2) dihedral angles. *J. Chem. Theory Comput.* 8:3257–3273.

57. Huang, J., and A. D. MacKerell, Jr. 2013. CHARMM36 all-atom additive protein force field: validation based on comparison to NMR data. *J. Comput. Chem.* 34:2135–2145.

58. Kumari, R., R. Kumar, A. Lynn; Open Source Drug Discovery Consortium. 2014. g_mmpbsa–a GROMACS tool for high-throughput MM-PBSA calculations. *J. Chem. Inf. Model.* 54:1951–1962.

59. Katritch, V., K. A. Reynolds, …, R. Abagyan. 2009. Analysis of full and partial agonists binding to beta2-adrenergic receptor suggests a role of transmembrane helix V in agonist-specific conformational changes. *J. Mol. Recognit.* 22:307–318.

60. Del Carmine, R., C. Ambrosio, …, T. Costa. 2002. Mutations inducing divergent shifts of constitutive activity reveal different modes of binding among catecholamine analogues to the beta(2)-adrenergic receptor. *Br. J. Pharmacol.* 135:1715–1722.

61. Del Carmine, R., P. Molinari, …, T. Costa. 2004. "Induced-fit" mechanism for catecholamine binding to the beta2-adrenergic receptor. *Mol. Pharmacol.* 66:356–363.

62. Strader, C. D., I. S. Sigal, …, R. A. Dixon. 1988. Conserved aspartic acid residues 79 and 113 of the beta-adrenergic receptor have different roles in receptor function. *J. Biol. Chem.* 263:10267–10271.

63. Suryanarayana, S., and B. K. Kobilka. 1993. Amino acid substitutions at position 312 in the seventh hydrophobic segment of the beta 2-adrenergic receptor modify ligand-binding specificity. *Mol. Pharmacol.* 44:111–114.

64. Ambrosio, C., P. Molinari, …, T. Costa. 2000. Catechol-binding serines of beta(2)-adrenergic receptors control the equilibrium between active and inactive receptor states. *Mol. Pharmacol.* 57:198–210.

65. Liapakis, G., J. A. Ballesteros, …, J. A. Javitch. 2000. The forgotten serine. A critical role for Ser-2035.42 in ligand binding to and activation of the beta 2-adrenergic receptor. *J. Biol. Chem.* 275:37779–37788.

66. Liapakis, G., W. C. Chan, …, J. A. Javitch. 2004. Synergistic contributions of the functional groups of epinephrine to its affinity and efficacy at the beta2 adrenergic receptor. *Mol. Pharmacol.* 65:1181–1190.

67. Strader, C. D., M. R. Candelore, …, R. A. Dixon. 1989. Identification of two serine residues involved in agonist activation of the beta-adrenergic receptor. *J. Biol. Chem.* 264:13572–13578.

68. Wieland, K., H. M. Zuurmond, …, M. J. Lohse. 1996. Involvement of Asn-293 in stereospecific agonist recognition and in activation of the beta 2-adrenergic receptor. *Proc. Natl. Acad. Sci. USA.* 93:9276–9281.

69. Bandaru, S., M. Alvala, …, S. K. Singh. 2017. Molecular dynamic simulations reveal suboptimal binding of salbutamol in T164I variant of β2 adrenergic receptor. *PLoS One.* 12:e0186666.

70. Isin, B., G. Estiu, …, Z. N. Oltvai. 2012. Identifying ligand binding conformations of the β2-adrenergic receptor by using its agonists as computational probes. *PLoS One.* 7:e50186.

71. Plazinska, A., M. Kolinski, …, K. Jozwiak. 2013. Molecular interactions between fenoterol stereoisomers and derivatives and the β_2-adrenergic receptor binding site studied by docking and molecular dynamics simulations. *J. Mol. Model.* 19:4919–4930.

72. Dickson, C. J., V. Hornak, …, J. S. Duca. 2016. Uncoupling the structure-activity relationships of β2 adrenergic receptor ligands from membrane binding. *J. Med. Chem.* 59:5780–5789.

73. Manna, M., W. Kulig, …, I. Vattulainen. 2015. How to minimize artifacts in atomistic simulations of membrane proteins, whose crystal structure is heavily engineered: β_2-adrenergic receptor in the spotlight. *J. Chem. Theory Comput.* 11:3432–3445.

74. Zocher, M., J. J. Fung, …, D. J. Müller. 2012. Ligand-specific interactions modulate kinetic, energetic, and mechanical properties of the human β2 adrenergic receptor. *Structure.* 20:1391–1402.

75. Cole, S. W., and A. K. Sood. 2012. Molecular pathways: beta-adrenergic signaling in cancer. *Clin. Cancer Res.* 18:1201–1206.